

New Antagonists of the Membrane Androgen Receptor OXER1 from the ZINC Natural Product Database

Athanasios A. Panagiotopoulos, Konstantina Kalyvianaki, George Notas, Stergios A. Pirintsos, Elias Castanas,* and Marilena Kampa*



Cite This: *ACS Omega* 2021, 6, 29664–29674



Read Online

ACCESS |



Metrics & More

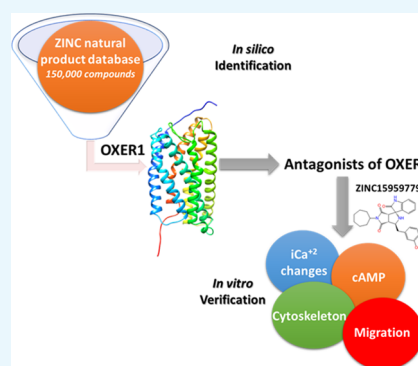


Article Recommendations



Supporting Information

ABSTRACT: OXER1 (oxoeicosanoid receptor 1) was deorphanized in 1993 and found to be the specific receptor for the arachidonic acid metabolite 5-oxo-EETE. Recently, we have reported that androgen binds to this receptor also, being a membrane androgen receptor, triggering a number of its membrane-mediated actions (cell migration, apoptosis, cell proliferation, Ca^{2+} movements). In addition, our previous work suggested that a number of natural monomeric and oligomeric polyphenols interact with OXER1, acting similar to testosterone. Here, we interrogated the natural product chemical space and identified nine polyphenolic molecules with interesting *in silico* pharmacological activities as putative OXER1 antagonists. The molecule with the best pharmacokinetic–pharmacodynamic properties (ZINC15959779) was purchased and tested on OXER1, in prostate cancer cell cultures. It showed that it has actions similar to those of testosterone in inhibiting cAMP, while it had no action in intracellular Ca^{2+} mobilization or actin cytoskeleton rearrangement/migration. These results are discussed under the prism of structure–activity relationships and *in silico* models of the OXER1 binding groove. We suggest that these compounds, together with the previously reported (poly)phenolic compounds, can be lead structures for the exploration of the anti-inflammatory and antiproliferative effects of OXER1 antagonists.



1. INTRODUCTION

In response to cellular stimuli, membrane phospholipids are hydrolyzed to generate intercellular messengers. Phospholipase A-2 (PLA₂) enzymes catalyze the hydrolysis of glycerophospholipid substrates to yield a free fatty acid and a 2-lysophospholipid.¹ Arachidonic acid, the product of such hydrolysis, is the precursor of a multitude of pro- and anti-inflammatory lipid mediators, such as prostaglandins, thromboxanes, and lipoxins through the cyclooxygenase (COX) pathway and leukotrienes through the lipoxygenase (LOX) pathway (see ref 2 and references herein). This multitude of mediators act through interactions with a number of G-protein-coupled receptors (GPCRs), mediating specific, usually proinflammatory, actions.³ Among the products of arachidonic acid catabolism, under the action of 5-LOX, are 5-OH or 5-oxo eicosanoids (5-HETE, 5,15-HETE, 5-oxo-EETE).^{4–10} Functional studies with these molecules revealed that 5-oxo-EETE acts through an interaction with a specific GPCR.^{11,12} Later on, GPR170 was deorphanized and found to be the specific receptor for 5-oxo-EETE, named OXER1.^{13,14}

OXER1 is a class A GPCR in the same classification branch as the leukotriene receptors.¹⁵ It is particularly expressed in inflammatory cells (eosinophils, neutrophils, lymphocytes, and monocytes), liver, kidney, spleen and pulmonary tissues, and cancer cells, including prostate and breast,⁴ and is considered as an inflammatory receptor, particularly implicated in

inflammatory pulmonary diseases and conditions like asthma. In this respect, the identification of antagonists of OXER1 might be a valuable therapeutic strategy in a multitude of diseases and conditions in which inflammation is an underlying mechanism.

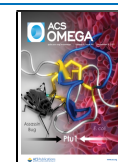
Recently, we have shown that OXER1 can also be a membrane testosterone receptor,⁶ expressed in a number of cell lines and tissue specimens of prostate and breast cancer.⁴ Testosterone antagonized the effect of 5-oxo-EETE on the inhibition of cAMP production by hindering G_{αi}-GDP binding on the ligand–receptor complex.¹⁶ In addition, previous results of our group^{16,17} have shown that natural polyphenols (catechin, epicatechin, and their natural dimers) interact with OXER1, eliciting antagonistic actions similar to those of testosterone (*in vitro* and *in vivo*). In this respect, these compounds could be good potential scaffolds for the selection, design, and development of novel OXER1 antagonists.

In view of the aforementioned data, we have interrogated chemical databases targeting natural products, and we have

Received: July 28, 2021

Accepted: September 13, 2021

Published: October 28, 2021



isolated and validated a number of compounds, which could represent potential antagonists of OXER1. We have taken advantage of a recently published tool,¹⁶ which can discriminate between the agonistic and antagonistic properties of different compounds, by integrating *in silico* binding to a GPCR and its interaction with $G\alpha$ proteins. By interrogating a large database of natural products, we have identified nine compounds and after an extensive *in silico* prediction of their pharmacological properties, we have tested the best candidate *in vitro*. We suggest that these compounds, together with the previously reported (poly)phenolic compounds,¹⁷ can be the lead compounds for the exploration of the anti-inflammatory and antiproliferative effects of OXER1 antagonists.

2. RESULTS

2.1. QSAR Modeling. In our previous work, we have initiated a tool that can predict the agonistic or antagonistic property of a given compound on a GPCR, based on the association of the $G\alpha$ -GDP interaction with the liganded GPCR.¹⁶ In the same publication, we have reported that a number of lipids, natural polyphenols, and synthetic steroids can be correctly classified as agonists, partial agonists, or antagonists on OXER1. Here, we have used validated polyphenol compounds on cAMP production (the final state of OXER1 activation⁶) as the training set, together with the prototype agonist (5-oxo-ETE) and antagonist (testosterone) and some proprietary steroid compounds (TC150-153)¹⁶, while a number of molecules we have previously analyzed were used as the validation set (Table 1). Further, we have

Table 1. Compounds Used for the Training and Prediction of the QSAR Models

training		prediction	
name	$G\alpha$ -interaction (kcal/mol)	name	$G\alpha$ -interaction (kcal/mol)
5-oxo-ETE	-896.5	5-HETE	-710.8
testosterone	-663	12-HpETE	-713.8
TC150	-657.3	15HpETE	-758.3
TC151	-645.2	12-HETE	-717.7
TC153	-635.2	15-HETE	-723.8
B2	-665.2	progesterone	-773.6
B5	-736.2	DHEA	-660.8
epicatechin	-642.8	TC404	-680.8
		TC405	-692
		TC406	-662.8
		TC407	-732.4
		B1	-676.6
		B3	-663.8
		B4	-682.9
		catechin	-669.2
		catechin_galate	-718.5
		epicatechin-3-O-gallate	-680.2
		epigallocatechin_gallate	-721.7

calculated 2D and 3D descriptors for these compounds using the PyMOL plugin PyDescriptor (10 946 descriptors).¹⁸ We have used the reported interaction of the receptor–ligand– $G_{\alpha i}$ -GDP as a response and the QSARINS program^{19–21} for the calculation of the best descriptors' equation.

Training molecules were selected from the list presented in ref 16. In this publication, a cutoff value of >-666 kcal/mol of liganded receptor- $G_{\alpha i}$ interaction was found to discriminate

antagonists from partial agonists. The antagonistic property of the training dataset was also verified by an intracellular cAMP assay, as described in the same reference.

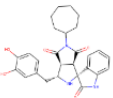
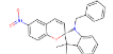
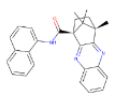
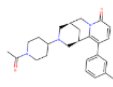
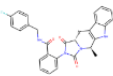
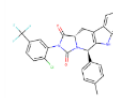
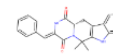
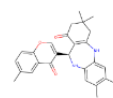
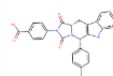
Following the details described in the Experimental Section, we have identified 65 models, which, after internal and external validation, were ranked according to the multicriteria decision making (MCDM),²² a technique summarizing the performances of internal and external validation criteria simultaneously, as a single number (score) between 0 and 1, where 0 represents the worst validation criteria value and 1 the best. The 10 best models were retained for further inspection.

Detailed analysis of the models and especially their loss of function (LOF), related to the number of selected variables, and Q_{LOO} , related to the performance of the model, together with the absence of correlation among the selected variables ($R^2 < 0.7$), led to the selection of models with 5–7 independent variables. However, as the number of training compounds was small (8) compared to the number of retained variables (99), a probability always exists that chance correlation could occur in the description of the model(s). We have therefore calculated 25 additional sets of the same set of molecules using the same variable selection procedure and randomized responses using the “permuted responses—original variables”²³ procedure of the QSARINS program. Indeed, for the retained models, there is a $>50\%$ probability at a $p < 0.05$ that chance correlation might exist. We have therefore scrutinized the selected models and retained the one with five independent descriptors, representing a physical and/or chemical entity compatible with the training dataset.

The finally retained model contains five unrelated variables (Figure S1A). Variables and validation of the model are further presented in Figure S1. The model predicts with a high accuracy the activity of compounds in the training set ($R^2 = 0.9999$, $R_{adj}^2 = 0.9999$, Figure S1B), while no outliers in the training set were detected, either with the model equation or by the leave-one-out (LOO) calculations. The choice of this model was based on the following: (1) the smallest number of descriptors describing correctly the activity of the training molecules. This results in an increased Q_{LOO}^2 (0.9991) and increased performance, as reflected by a very small lack-of-fit (LOF) value (1.75). (2) The independence of retained descriptors (descriptor intercorrelation index $K_{xx} = 0.48$, one of the smallest values among examined models). (3) The very small difference between the correlation coefficient (R^2) and the correlation after leaving one variable out (Q_{LOO}^2) ($\Delta R^2 - Q_{LOO}^2 = 0.0007$; see also the green and blue dots in Figure S1B). (4) The calculated values of the training set are well concentrated within a small space, discriminating among the different chemical families (Figure S1D,E), determining also the applicability domain of the model, as shown in the Insubria graph²⁴ presented in Figure S1C.

2.2. Selection of Compounds with Potential Antagonistic Properties on OXER1. **2.2.1. ChEMBL Database.** In the first step, we interrogated the ChEMBL database of bioactive molecules with drug-like properties (<https://www.ebi.ac.uk/chembl>,^{25,26}) for substances active on the OXER1 molecule. Eighty compounds were retrieved; their molecular descriptors were calculated with PyDescriptor, and their predictive agonistic/antagonistic activity was calculated with QSARINS, based on the retained model (see the previous paragraph). The calculated activity (expressed in ΔG) was returned, together with the leverage value of each chemical. We then selected substances, within the applicability domain of

Table 2. List of the Retained Natural Compounds from the ZINC12 Database, Acting as Potential Antagonists on OXER1

Name	Chemical Structure	kcal/mol			Formula	MW	Canonical SMILES
		Pred. Binding to OXER1	Predicted interaction with $G_{\alpha i}$	Pred. by QSAR			
ZINC15959779		-19.655	-662.44	-661.7837	C27H29N3O5	475.54	<chem>O=C1N(C2CCCCC2)C(=O)[C@@H]2[C@H]1[C@@H](Cc1ccc(c(c1)O)O)N[C@@]12C(=O)Nc2c1cccc2</chem>
ZINC02274955		-15.579	-661.12	-662.2376	C25H22N2O3	398.45	<chem>[O-][N+](=O)c1ccc2c(c1)C=C[C@@]1(O2)N(Cc2cccc2)c2c(C1(C)C)ccc2</chem>
ZINC01805555		-14.867	-663.94	-639.4079	C27H25N3O	407.51	<chem>O=C([C@]12CC[C@@](C2(C)C)(c2c1nc1cccc1n2)C)Nc1cccc2c1ccc2</chem>
ZINC05397075		-15.412	-656.03	-669.4895	C25H28N4O2	416.52	<chem>N#Cc1cccc(c1)c1ccc(=O)n2c1[C@@H]1C[C@H](C2)CN(C1)C1CCN(CC1)C(=O)C</chem>
ZINC08790433		-18.312	-664.7	-670.9441	C28H23FN4O3	482.51	<chem>Fc1ccc(cc1)CNC(=O)c1cccc1N1C(=O)[C@H]2N(C1=O)[C@H](C)c1c(C2)c2cccc2[nH]1</chem>
ZINC12864636		-18.122	-659.28	-660.6397	C27H19ClF3N3O2	509.91	<chem>Cc1ccc(cc1)[C@H]1N2[C@@H](Cc3c1[nH]c1c3cccc1)C(=O)N(C2=O)c1cc(ccc1Cl)C(F)(F)F</chem>
ZINC02121631		-15.673	-664.77	-666.8884	C23H21N3O2	371.43	<chem>O=C1N/C(=C/c2cccc2)/C(=O)N2[C@H]1Cc1c3cccc3[nH]c1C2(C)C</chem>
ZINC04081886		-16.925	-660.97	-645.0612	C27H28N2O3	428.52	<chem>Cc1ccc2c(c1)c(=O)c(co2)[C@@H]1Nc2cc(C)c(cc2NC2=C1(=O)CC(C2)(C)C</chem>
ZINC12881427		-18.599	-665.69	-665.897	C27H21N3O4	451.47	<chem>Cc1ccc(cc1)[C@@H]1N2[C@@H](Cc3c1[nH]c1c3cccc1)C(=O)N(C2=O)c1ccc(cc1)C(=O)O</chem>

the model (ΔG between -600 and -700 kcal/mol, as we are searching for OXER1 antagonists, and the cutoff value of an antagonist is > -666 kcal/mol¹⁶ and the cutoff value of HAT is $h' = 2.25$ ²⁷). Although all molecules showed predictive $\Delta G_s > -500$ kcal/mol, none fell inside the applicability domain of our model. This is expected, as the reported compounds were tested as antagonists of OXER1 in another system (human peripheral neutrophils) and function (inhibition of intracellular Ca^{2+}),^{28,29} as compared to our model, describing the interaction of compounds with $G_{\alpha i}$ proteins and modification of cAMP production.

2.2.2. ZINC Database. We applied the retained model on all ZINC natural products database ($\sim 150\,000$ compounds,

<http://zinc.docking.org/>³⁰) after calculation of their molecular descriptors. Application of the retained model (see above) to these compounds, with a HAT* cutoff value $h' = 2.25$ as above and a predicted G_{α} -GDP affinity between -670 and -600 kcal/mol, returned nine compounds that comply with the selection criteria imposed, concerning the applicability domain of our model (Table 2) and further assayed *in silico*, as described below.

The table provides the ZINC database identification number, the 2D compound formula, its predicted interaction with OXER1 in a fully flexible model, the interaction of liganded OXER1 with $G_{\alpha i}$, the predicted interaction from the application of the retained QSAR model, its formula, molecular

weight, and canonical SMILES. Note that according to a previous work from our group,¹⁶ a liganded receptor- G_{ai} interaction > -666 kcal/mol classifies the compound as an antagonist. As shown in the list, all retained compounds are potent antagonists.

2.3. Drugability of the Retained Natural Compounds.

As presented in Table 2, we found a very good match between the QSAR-identified and the predicted interaction of the nine identified compounds on OXER1. All identified substances bind with high affinity to OXER1, with a calculated ΔG between 14.9 and 19.7 kcal/mol. In addition, the predicted interaction of the liganded OXER1 with the G_{ai} protein presents a ΔG between 660 and 665 kcal/mol, identifying them as OXER1 antagonists.¹⁶

Using the online resource SwissADME (www.swissadme.ch),³¹ we further calculated some parameters useful for the drugability of the retained compounds (Table 3; see Table S1 for the whole list of criteria). As shown, all compounds are predicted to penetrate the gastrointestinal (GI) barrier, which provides them with an advantage compared to the previously identified antagonist B2-OPC.^{16,17} In addition, with the exception of ZINC12864636, they do not violate Lipinski's rule of five,^{32,33} suggesting that they are good drugable candidates. However, all of the retained compounds interact with a number of drug-metabolizing enzymes (Table 3) and are predicted to interact with a number of receptors or other proteins (Table S2), according to the online resource Similarity Ensemble Approach (SEA, <https://sea.bkslab.org/>),³⁴ including ion channels and neurotransmitter receptors. Concerning drug transporters and drug-metabolizing enzymes, the compounds with the lower interactions are ZINC15959779, predicted to interact with P-glycoprotein (MDR1, ABCB1) and to inhibit CYP2D6 and ZINC12864636, inhibiting CYP2C9 and CYP2C19. Furthermore, compound ZINC15959779 does not present any notable interaction with human protein targets (at the threshold of $p < 1^{-10}$ applied here), while ZINC12864636 interacts with Krebs's cycle enzymes, RB1 protein, and cyclic nucleotide phosphodiesterases (Table S2).

Based on this information, we retained compound ZINC15959779 as the most prominent candidate as a lead molecule inhibiting the action of OXER1 and tested its conformational matching with other OXER1 antagonists and its *in vitro* activity.

2.4. Structure–Activity Relationship of ZINC15959779 on OXER1. Simulations performed on online resources as full flexible binding on specific macromolecules necessitate a computing power not available *in situ*; especially for noncrystallized molecules, they have a number of inherent dangers and should be validated extensively. In our case, the majority of simulations were performed on the Galaxy server³⁵ using a truncated form of the OXER1 receptor, lacking 70 extracellular amino acids and the totality of the intracellular helix 8. Very recently, the AlphaFold initiative^{36,37} produced a more detailed structure of a large number of proteins available at <https://alphafold.ebi.ac.uk/>. We retrieved the proposed structure of OXER1 (code Q8TDSS) and compared it with our retained model. Minor differences were observed between the two models. Performing a fully flexible binding of the new provided model in the Galaxy server provided the same structure of the binding pocket (Table S1). Interestingly, using the COACH server,³⁸ we obtained the same amino acid residues involved in testosterone binding to OXER1,

Table 3. Predicted Physicochemistry, Drug-likeness, Pharmacokinetics, and Medicinal Chemistry Properties of Retained Compounds^a

name	formula	MW	#HA	#AHA	#RB	#HBA	#HBD	MR	iLOGP	ESOL	ESOL class	GI-abs	BBB	Pgp	1A2-i	2C19-i	2C9-i	2D6-i	3A4-i	#viol
ZINC15959779	$C_{27}H_{29}N_3O_5$	475.54	35	12	3	6	4	140.23	3.13	2.77×10^{-5}	M	H	N	Y	N	N	Y	N	N	0
ZINC02274955	$C_{25}H_{22}N_2O_3$	398.45	30	18	3	3	0	123.27	3.19	3.16×10^{-7}	P	H	Y	N	Y	Y	Y	N	Y	0
ZINC01805555	$C_{27}H_{25}N_3O$	407.51	31	20	3	3	1	124.93	3.59	1.18×10^{-6}	M	H	Y	Y	Y	Y	Y	Y	Y	0
ZINC05397075	$C_{25}H_{28}N_4O_2$	416.52	31	12	3	4	0	127.44	3.19	3.03×10^{-4}	S	H	Y	Y	N	N	Y	Y	Y	0
ZINC08790433	$C_{28}H_{33}FN_4O_3$	482.51	36	21	5	4	2	140.13	3.38	4.19×10^{-6}	M	H	N	Y	Y	Y	Y	Y	Y	0
ZINC12864636	$C_{27}H_{19}ClF_3N_3O_2$	509.91	36	21	3	5	1	137.34	3.71	7.44×10^{-8}	P	H	N	N	N	Y	Y	N	N	2
ZINC02121631	$C_{23}H_{21}N_3O_2$	371.43	28	15	1	2	2	116.27	2.93	2.76×10^{-5}	M	H	Y	Y	Y	Y	Y	Y	Y	0
ZINC04081886	$C_{27}H_{28}N_2O_3$	428.52	32	16	1	3	2	135.24	3.88	1.17×10^{-6}	M	H	Y	Y	N	Y	Y	N	Y	0
ZINC12881427	$C_{27}H_{21}N_3O_4$	451.47	34	21	3	4	2	134.29	2.88	2.90×10^{-6}	M	H	N	Y	N	Y	Y	N	N	0
Testosterone	$C_{19}H_{28}O_2$	288.42	21	0	0	2	1	85.36	2.9	1.91×10^{-4}	S	H	Y	N	N	N	N	N	N	0
B2-OPC/ZINC3954422	$C_{30}H_{26}O_{12}$	578.52	42	24	3	12	10	146.71	1.35	7.17×10^{-6}	M	L	N	N	N	N	N	N	Y	3

^aTable presents parameters, calculated with the SwissADME online resource,³¹ related to the solubility, absorption, distribution, and interaction with drug-metabolizing enzymes of the retained compounds. Testosterone and B2-OPC are also provided for comparison. Abbreviations: #HA, number of heavy atoms; #AHA, number of aromatic heavy atoms; #RB, number of rotatable bonds; #HBA, number of H-bond donors; #HBD, number of H-bond acceptors; #HBD, number of H-bond donors; ESOL, solubility in mol/L; M, moderately soluble; P, poorly soluble; S, soluble; GI-abs, gastrointestinal absorption; H, high; L, low; BBB-perm, blood–brain barrier permeant; Y, yes; N, no; Pgp, P-glycoprotein substrate; #viol, number of violations of Lipinski's rule of five. Cytochrome inhibitor status designated as {CYP subtype}-i, for example, 1A2-i indicates CYP1A2 inhibitor.

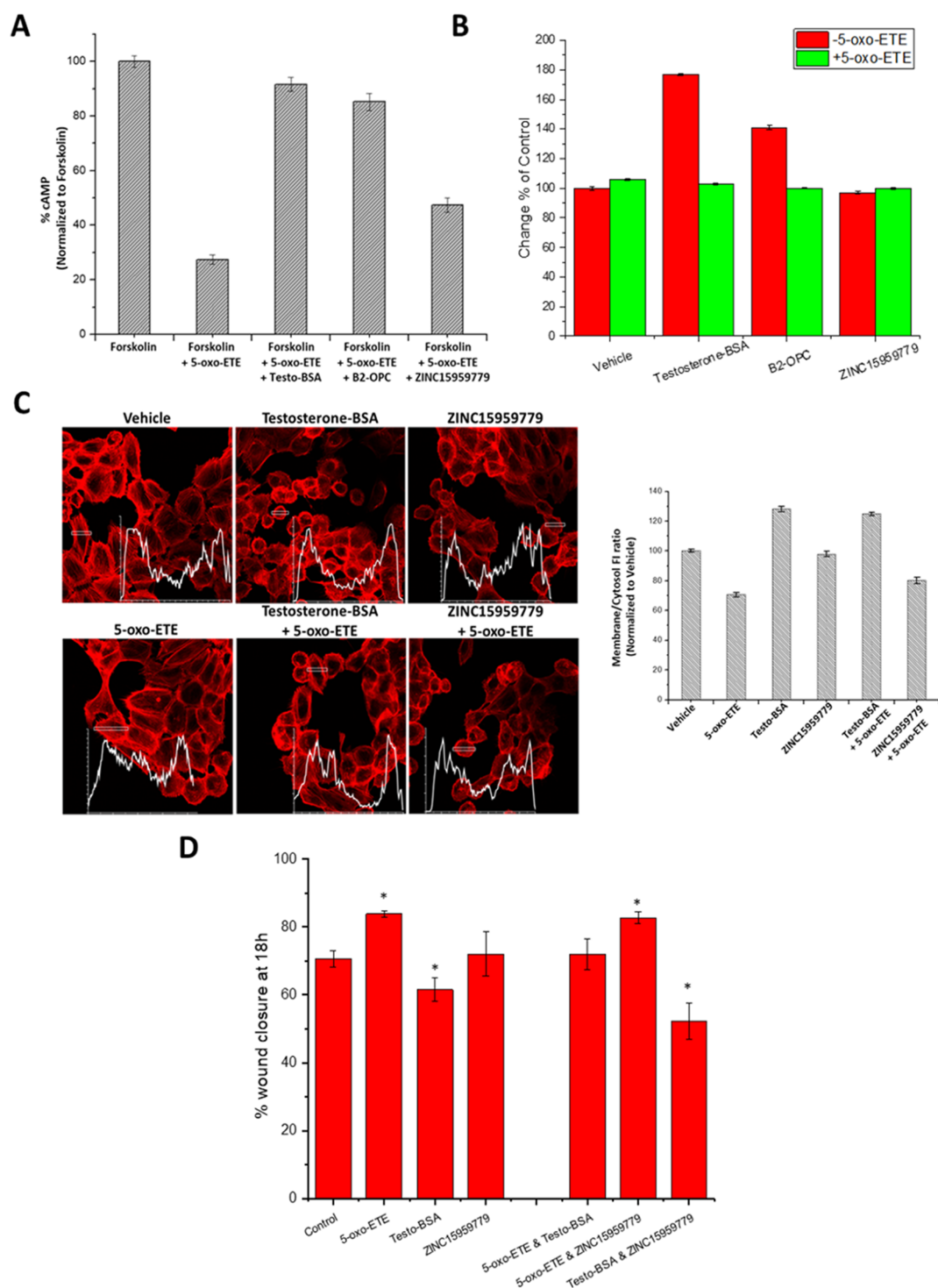


Figure 1. Cellular effects of ZINC15959779. (A) 5-Oxo-EETE, the natural agonist of OXER1, inhibits the forskolin-induced cAMP cellular production in DU-145 cells. Testosterone-BSA⁶ and B2-OPC¹⁶ inhibit this effect, a result shared by ZINC15959779. Mean \pm SE of three separate experiments in triplicate. (B) Intracellular Ca²⁺ levels in DU-145 prostate cancer cells treated with different antagonists in the absence (red bars) or the presence of the agonist 5-oxo-EETE (blue bars). Mean \pm SE of three different experiments. Please also refer to Figure S2 for a kinetic experiment of Ca²⁺ changes. (C) Actin cytoskeleton changes of DU-145 cells after incubation in the denoted conditions in each panel for 20 min. Actin was stained with rhodamine-phalloidin and visualized in a confocal microscope. In each panel, a densitometric curve of actin distribution is also presented, which served for the calculation of peripheral (membrane) to intracellular actin distribution, as shown in the right panel (mean \pm SE of the measurement of at least 10 cells). (D) Wound healing (cell migration) assay in the presence of the agonist (5-oxo-EETE), antagonist (testosterone), or ZINC15959779 (all at 10⁻⁶ M) alone or in combination with the agonist. Mean \pm SE of three different experiments performed in duplicate and normalized as per control. Please refer to Figure S4 for a typical result. The figure presents data at 18 h, while similar results were obtained at 24 h.

confirming the validity of our approach. The interaction of ZINC15959779 with OXER1 occurred at the same binding pocket, interacting with the same amino acid residues, as detailed in the Supporting Information (Table S1, Figures S6 and S7). The table presents parameters calculated with the SwissADME online resource³¹ related to the solubility, absorption, distribution, and interaction with drug-metabolizing enzymes of the retained compounds. Testosterone and B2-OPC are also provided for comparison.

2.5. In Vitro Testing of the Selected Compound. In Figure 1, the *in vitro* effects of the best-retained compound, ZINC15959779, in DU-145 cells are shown. The compound reverts the inhibition of cAMP production induced by 5-oxo-ETE, being about twofold less potent than testosterone-BSA (a testosterone analogue interacting exclusively at the membrane level) and B2-OPC (Figure 1A). This result confirms the potency of the applied QSAR and selection criteria imposed here in identifying OXER1 antagonists based on $G_{\alpha i}$ selection criteria. ZINC15959779 could not induce intracellular calcium changes, in contrast to those reported for testosterone (Panagiotopoulos et al.¹⁶), related to a $G_{\beta\gamma}$ interaction, in contrast to testosterone-BSA and B2-OPC (Figures S2 and S9B). Additionally, no apparent changes of the actin cytoskeleton were observed under ZINC15959779 (Figure 1C; see also Figure S3, for higher magnification). Indeed, as reported previously,^{6,17,39} testosterone-BSA induces a sub-membrane localization of polymerized actin and reduction of intracellular stress fibers induced by 5-oxo-ETE, an effect mimicked by B2-OPC, leading to a redistribution of intracellular actin, an action not repeated by ZINC15959779 (Figure 1C). The polymerized actin cytoskeleton rearrangements lead to a reduction of cell migration and induction of apoptosis by testosterone-BSA as previously reported,^{17,39} which is not reverted by 5-oxo-ETE. Contrariwise, ZINC15959779 had no apparent effect on migration at 18 h (Figures 1D and S4) or 24 h (not shown) of treatment. These phenotypic changes are related to $G_{\beta\gamma}$ signal transduction.⁶ In this respect, ZINC15959779 is a pure $G_{\alpha i}$ antagonist on OXER1, while it has no effect on $G_{\beta\gamma}$ -related actions of the receptor.

3. DISCUSSION

OXER1, the receptor of the oxidized arachidonic acid metabolite 5-oxo-ETE,^{4–9,40,41} emerged recently as a potential target in inflammatory diseases and cancer. Indeed, the activation of OXER1 increases cell migration^{11,12} and promotes cancer cell survival,^{42,43} while its antagonists decrease inflammatory elements and decrease cancer cell migration, initiating apoptosis.^{6,17,44} In this respect, a search of OXER1 antagonists might be a valuable target for novel anti-inflammatory and/or cancer therapeutics. Previous research has identified a number of indole derivatives as OXER1 inhibitors of calcium mobilization and neutrophil chemotaxis,^{28,29} while our group has proposed membrane-acting testosterone and B2-OPC as inhibitors of OXER1, with beneficial effects in prostate cancer control.^{6,16,17}

In the present study, we interrogated the chemical space of natural products in search of better OXER1 antagonists. The novel inhibitors should have advantages over previously identified conjugated steroids⁶ and polyphenols,¹⁷ being devoid from the side effects of steroids, such as testosterone, and having a better gastrointestinal permeability, permitting their *per os* administration. In our search, we have taken

advantage of a recent tool¹⁶ that integrates *in silico* the ligand–receptor binding with the interaction of the liganded receptor with G-proteins, permitting the distinction of agonists and antagonists of a given GPCR. This tool has been developed with a wide array of known GPCR ligands and receptors and validated with OXER1 known agonists and antagonists.

Interrogating the ZINC database of natural products, with a stringent use of QSAR methodology,⁴⁵ we have identified nine compounds as potential OXER1 antagonists. They possess interesting properties, including good gastrointestinal (GI) permeability. Some of them are also substrates of P-glycoprotein, a multidrug resistance protein (MDR) that ensures the transport of substances from the cytosol to the extracellular space,^{46,47} thereby ensuring interaction with the membrane OXER1 and enhancing their action. Others are inhibitors of CYP2C9 implicated in arachidonic acid metabolism,⁴⁸ providing another layer of antagonism by inhibiting the synthesis of the endogenous ligand. Finally, all of the identified compounds interact with diverse drug-metabolizing enzymes.

Identified compounds or their structural isomers have been previously assayed in different systems. Some of them possess antitumor activities compatible with our previous data on the effect of OXER1 antagonists on cancer.^{6,17,44,49–51} A chromophenazine structural isomer of ZINC02274955 was isolated from *Streptomyces* sp. Ank 315⁵² and displays a broad range of activities as an antioxidant, neuroprotectant, broad-spectrum antimicrobial, antiparasitic, antiviral, antitumor, and antimalarial agent.^{53,54} A structural isomer of ZINC04081886 (AdipoRon) was used as an adiponectin receptor (Adipo 1 and 2) agonist, improving lipid metabolism,⁵⁵ inhibiting steroidogenesis⁵⁶ and inducing tumor suppression *in vitro* and *in vivo*.^{57–59} Finally, a structural isomer of ZINC12881427 from the *Streptomyces longisporoflavus* strain inhibited protein kinase C with IC_{50} values in the micromolar range,⁶⁰ contrasting the effect of 5-oxo-ETE, which activates this kinase.⁶

From the pharmacokinetics and drugability evaluation of the nine compounds, we have retained ZINC15959779, which presented the most favorable profile. A structural isomer of this compound presents a remarkable growth inhibitory activity of a number of cancer cell lines, including NSCLC, breast, and renal cancer cell lines.⁶¹ In our hands, ZINC15959779 exhibited a selective $G_{\alpha i}$ antagonism on OXER1, not interfering with $G_{\beta\gamma}$ -related functions. This result pinpoints the robustness and the selectivity of the applied approach (i.e., the interrogation of the $G_{\alpha i}$ -related potency of compound-liganded OXER1) and confirms the opinion advanced by experts in the field that QSAR should be used with care and all of the necessary precautions and validation steps.^{24,27,45}

The use of *in silico* methods to determine the bonds that develop between a ligand and a receptor requires special care because of the different approaches followed by different programs. In our approach, we used two different servers (Galaxy³⁵ and COACH³⁸), two different predicted OXER1 pdb files (the truncated one used in our previous publications and the one predicted by the AlphaFold consortium^{36,37}), and two alignment methods (GemDock⁶² and Discovery Studio). The identified ZINC15959779 compound binds at the same pocket as 5-oxo-ETE and testosterone and forms similar bonds as the other antagonists. However, as shown, ZINC15959779 forms additional bonds, explaining its higher simulated affinity for the receptor. In addition, a detailed analysis of $G_{\alpha i}$ -related functions (for example, inflammation enhancement through an

increased JNK- and p38 α -enhanced activation by 5-oxo-EETE and the subsequent inhibition by OXER1 antagonists we have previously reported,⁶ or the inhibition of NF κ B activity by CREB phosphorylation (see ref 63 for a recent review and references herein)) and the specific effects of OXER1 antagonists through G $\beta\gamma$ on Ca²⁺ (Panagiotopoulos et al.¹⁶) and cell migration⁶ would permit the design of specific G α_i - and G $\beta\gamma$ -specific inhibitors applying the methodology presented here, a work currently in progress.

In conclusion, in the present study, by a thorough application of QSAR methods in the natural products chemical space, we have identified a small number of molecules with G α_i antagonistic properties on the OXER1 receptor. The application of this methodology with proper *in vitro* validation might permit the design of novel anti-inflammatory and/or anticancer agents. Finally, our applied methodology might be useful for the identification of specific agonists/antagonists of other GPCRs.

4. EXPERIMENTAL SECTION

4.1. Determination (*In Silico*) of Binding Affinity and G α_i -GDP Binding of Selected Natural Products on OXER1. The simulation of the natural ligand 5-oxo-EETE, the natural antagonist testosterone, and a series of natural polyphenols on OXER1 was performed, as described in detail in a recent publication of our group.¹⁶ In brief, modelization of the OXER1 receptor was performed in the Swiss Model Biospace (<http://swissmodel.expasy.org/interactive>),^{64,65} while ligand structures were downloaded from the ZINC12 database (<http://zinc.docking.org/>)³⁰ in the canonical SMILES format and translated in pdb files with Open Babel (<http://openbabel.org>).⁶⁶ Fully flexible ligand–receptor binding was performed in the GalaxyWEB (<http://galaxy.seoklab.org>) online server,³⁵ with the specific program Galaxy7TM, followed by the final relaxation and refinement of the complex.^{67,68} The results reported the change of Gibbs free energy (ΔG in kcal/mol) and the ligand–receptor final pose in the pdb format, which was visualized with the UCSF Chimera program.⁶⁹ The same steps were followed for the generation of the G α_i -GDP complex. Finally, the two heteroprotein complexes were introduced in the HEX 8.0.8 program (<http://hex.loria.fr/>),⁷⁰ and the best solution of G α_i -GDP liganded to the OXER1-ligand complex in intracellular loops 2 and 3 was retained, together with the corresponding ΔG . According to our previous data,¹⁶ an interaction with a $\Delta G > -666$ kcal/mol indicates an antagonistic property of a given ligand.

4.2. Detection (*In Silico*) of the Interacting Amino Acids in the OXER1 Binding Pocket for Testosterone and Polyphenols. The identified structured OXER1 molecule in the pdb format was introduced in the GalaxyWEB server, as detailed above, together with the agonistic molecule (5-oxo-EETE) and the identified antagonists, testosterone and B2-OPC.¹⁶ The best returned solutions were analyzed with the PyMOL V2.4 program (Schrodinger.com). Amino acids with a distance ≤ 4.5 Å from any part of the ligand were retained. The receptor–ligand complex was hydrated in the GalaxyWEB server with the routine GalaxyWater-wKGB,⁷¹ and hydrogen bonds formed without or with intermediate water molecules were detected in PyMOL. In a second approach, OXER1 (in the FASTA format) was introduced in the COACH server (<https://zhanggroup.org/COACH/>),³⁸ which returned the interacting amino acids using a completely different algorithm.

The same data were repeated (on the Galaxy server) with the OXER1 conformation produced by AlphaFold (<https://alphafold.ebi.ac.uk/entry/Q8TDSS>).^{36,37}

4.3. QSAR Analysis. The training and prediction compounds (Table 1), as well as the compounds downloaded from the ZINC12 database, were introduced in the PyDescriptor add-on to the PyMOL program,¹⁸ and 10 945 molecular descriptors were calculated for each compound. These descriptors were then introduced in the QSARINS (V2.2.4) Quantitative Structure–Activity Relationship program,^{19,21} together with the calculated “activity” of each compound, represented by the ΔG (in kcal/mol) of the liganded receptor-G α_i -GDP binding (see Table 1 for details), as the target of the QSAR analysis.

In the first step, we excluded variables presenting a constant value (at a level of 80%) and correlated variables at a level of 95%. A total of 10 846 variables were excluded, while 99 variables were retained. QSAR was performed with the whole set of variables until 1, with 50 models per size using the Q_{LOO}² parameter (correlation coefficient after the leave-one-out cross-validation) as a fitness function to be minimized, at a significance level of 0.05, applying a QUIK rule of 0.050. The QUIK rule⁷² automatically excludes models in which the correlation between the block of the descriptors and the response (Kxy) is lower than or too similar to the intercorrelation among the descriptors (Kxx). This was followed by a robust optimization genetic algorithm, an advanced technique that mimics Darwinian evolution for variable selection.^{73,74} Parameters for the genetic algorithm were the number of variables up to 10, a population size of 100, and a mutation rate of 50, with 500 iterations per size. In addition, models with a ratio between the interval of confidence and the coefficient of one of the model descriptors greater than 1 were further eliminated. Criteria for the selected model are presented in the results section.

The leave-many-out (LMO) internal validation was performed with 2000 iterations and 30% of predicted compounds, while Y-scramble was also done with 2000 iterations.

4.4. In Vitro Tests. To validate our *in silico* data, we performed the following assays:

4.1.1. cAMP Production in DU-145 Human Prostate Cancer Cells. cAMP production in DU-145 human prostate cancer cells bearing OXER1 was assayed according to our previous report.⁶ The cells (from Braunschweig, Germany) were cultured in RPMI-1640 culture medium supplemented with 10% fetal bovine serum (FBS) at 37 °C and 5% CO₂. All media were purchased from Invitrogen (Carlsbad) and all chemicals from Merck (Darmstadt, Germany) unless otherwise stated. 5-Oxo-EETE (5-oxo-(6E,8Z,11Z,14Z)-6,8,11,14-eicosa-tetraenoic acid) was purchased from Tocris, U.K. Testosterone, B2-OPC, and epicatechin were purchased from Merck, and ZINC15959779 (the best compound selected from the list of identified molecules; see the Results section) was purchased from MolPort (Riga, Latvia).

OXER1 is coupled to a G α_i G-protein, inhibiting the production of cAMP, upon activation.⁶ Therefore, the cyclic adenosine monophosphate (cAMP) production after OXER1 stimulation by 5-oxo-EETE (10⁻⁷ M) alone, or in the presence of testosterone or the compounds under investigation (10⁻⁶ M, see the Results section) was examined, with a gain-of-signal competitive immunoassay (Promega cAMP Glo TM, Madison, WI). Since OXER1 is a G α_i -coupled receptor, forskolin (15

μM) was used to stimulate cAMP production and reveal the inhibitory effect of 5-oxo-ETE. The antagonistic effect of testosterone and other agents was assayed by pretreating cells with the different compounds at a concentration of 10^{-6} M for 15 min at 37°C , prior to the addition of 5-oxo-ETE, and cAMP was further assayed. The produced luminescence signal was read in a microplate fluorescence reader (Bio-Tek Instruments Inc. Winooski, Vermont). The results were expressed as % reversion of the 5-oxo-ETE effect in the presence of forskolin (see refs 6, 16 for details).

4.1.2. Intracellular Calcium Levels. DU-145 cells were seeded in 25 cm^3 culture flasks. After 24 h, the cells were detached from culture flasks by vigorous shaking, washed, and resuspended in Ca^{2+} medium (140 mM NaCl, 5 mM KCl, 1 mM MgCl_2 , 2 mM CaCl_2 , 10 mM HEPES (*N*-(2-hydroxyethyl)piperazine-*N'*-(2-ethanesulfonic acid)), 5 mM D-glucose) at a cell density of 0.5 million per mL. Subsequently, they were incubated for 30 min at 37°C in the dark with $5\ \mu\text{M}$ Fluo-4AM (Abcam, ab241082), centrifuged (1500xg, 10 min, RT), resuspended in calcium-free media (without calcium ions plus 1 mM EGTA, the final concentration of calcium ions is less than 0.1 nM), and transferred to quartz cuvettes. Fluorescence was measured at time intervals of 10 sec at a single excitation wavelength (488 nm) and a single emission wavelength (510 nm) with a PerkinElmer LS-3B fluorescence spectrometer. Cytosolic calcium ion responses were expressed as the peak fluorescence intensities (measured at 510 nm) produced by Fluo-4 using an excitation wavelength of 488 nm. Therefore, changes in calcium concentration are expressed as changes in fluorescence units.

4.1.3. Visualization of the Actin Cytoskeleton. DU-145 cells were seeded at an initial of 20 000 cells/well in an 8-well chamber slide with $250\ \mu\text{L}$ of medium per well. After 24 h, the cells were fixed with 4% paraformaldehyde in PBS for 10 min. Then, the cells were permeabilized with Triton X-100 0.2% w/v for 10 min. The cells were incubated with 2% BSA in PBS for 15 min, followed by staining with Rhodamine-labeled phalloidin (R415, Invitrogen) for 45 min at room temperature. Fixed-stained cells were mounted with Vectashield and observed on an inverted confocal scanning microscope (Leica SP2) using a $63\times$ objective lens with oil immersion and counterstained with DAPI (blue) to delineate the nuclear space. Actin intensities were then quantified using Image J software (<https://imagej.nih.gov/>).^{6,17}

4.1.4. Cell Migration Assay. DU-145 cells were cultured in RPMI-1640 with 10% v/v FBS at 24-well bottom plates. The cells were incubated at 37°C and 5% CO_2 . Confluent monolayers of the cells were treated with mitomycin C (10 mg/mL) for 2 h, to inhibit cell proliferation. Then, the medium with mitomycin C was removed and two straight lines were scratched in the monolayers, per well, with a micropipette tip to create a wound area. After that, the cells were treated with compounds (in 10^{-6} M). After the compounds were added, the initial images of the scratches under an inverted phase-contrast microscope (Vert.A1 ZEISS International, Jena, Germany) were acquired (time = 0). Series of images were obtained after 18 and 24 h of incubation at 37°C , to assay the rate of colonization of the denuded area. The magnitude of the wound area was measured at the time reported in Figures and normalized differences in migration (as % of control, nontreated cells).⁶ All assays were performed in DMSO +

ethanol in view of the different solubility characteristics of the different effectors.

4.5. Purity Statement. All compounds used were >95% pure by HPLC.

4.6. Statistical Methods. Statistical evaluation was performed by SPSS (IBM, Chicago, IL), Origin Pro 2018 (OriginLab, Northampton, MA), or GraphPad Prism V8 software (San Diego, CA), as appropriate. The statistical threshold was set to $p < 0.05$.

■ ASSOCIATED CONTENT

SI Supporting Information

The Supporting Information is available free of charge at <https://pubs.acs.org/doi/10.1021/acsomega.1c04027>.

In silico structure–activity relationships of OXER1 antagonists in the binding pocket of OXER1; predicted hydrogen bonds in the binding pocket of OXER1 formed by agonist and antagonists; absorption, distribution, metabolism, and excretion (ADME) values calculated with the online resource www.swissadme.ch; Similarity ensemble approach of the retained molecules (SEA); molecular descriptors of the retained QSAR model; effect of ZINC15959779 on intracellular Ca^{2+} release; high magnification of the actin cytoskeleton of DU-145 cells treated with 10^{-6} M of the different compounds for 30 min; microphotographs of an experiment of wound healing; conformations of the OXER1 binding pocket; and alignment of ZINC15959779 with testosterone and B2-OPC in the binding pocket of OXER1 (PDF)

■ AUTHOR INFORMATION

Corresponding Authors

Elias Castanas – Laboratory of Experimental Endocrinology, School of Medicine, University of Crete, Heraklion 715 00, Greece; Email: castanas@uoc.gr

Marilena Kampa – Laboratory of Experimental Endocrinology, School of Medicine, University of Crete, Heraklion 715 00, Greece; orcid.org/0000-0002-6324-9570; Email: kampam@uoc.gr

Authors

Athanasios A. Panagiotopoulos – Laboratory of Experimental Endocrinology, School of Medicine, University of Crete, Heraklion 715 00, Greece

Konstantina Kalyvianaki – Laboratory of Experimental Endocrinology, School of Medicine, University of Crete, Heraklion 715 00, Greece

George Notas – Laboratory of Experimental Endocrinology, School of Medicine, University of Crete, Heraklion 715 00, Greece

Stergios A. Pirintsos – Department of Biology, School of Science and Technology, University of Crete, Heraklion 71013, Greece; Botanical Garden, University of Crete, Rethymnon 700 13, Greece

Complete contact information is available at: <https://pubs.acs.org/doi/10.1021/acsomega.1c04027>

Author Contributions

Conceived and designed the study: M.K. and E.C.; performed the analyses and experiments: A.A.P. and K.K.; participated in its design and coordination and helped to draft the manuscript:

G.N. and S.A.P.; wrote the paper: M.K. and E.C. All authors read and approved the final manuscript.

Notes

The authors declare no competing financial interest.

ACKNOWLEDGMENTS

This work was partially supported by the Hellenic Foundation for Research and Innovation (H.F.R.I.) under the “First Call for H.F.R.I. Research Projects to support Faculty members and Researchers and the procurement of high-cost research equipment grant” (Project Number: 3725 to M.K.) and by Greece and the European Union (European Social Fund- ESF) through the Operational Programme “Human Resources Development, Education and Lifelong Learning” in the context of the project “Strengthening Human Resources Research Potential via Doctorate Research” (MIS-5000432), implemented by the State Scholarships Foundation (IKY) to AAP (Ph.D. scholarship). The authors also thank Professor Paola Gramatica for making the QSARINS program available to us.

ABBREVIATIONS USED

GPCR	G-protein-coupled receptor
ΔG	difference in Gibbs free energy
GDP	guanosine diphosphate
OXER1	oxoeicosanoid receptor 1
5-oxo-ETE	5-oxo-6E,8Z,11Z,14Z-eicosatetraenoic acid
pdB	protein data bank
$G_{\alpha i}$	inhibitory G α subunit
$G_{\beta\gamma}$	G β - γ subunit
B2-OPC	B2 proanthocyanidin

REFERENCES

- Dennis, E. A. The growing phospholipase A2 superfamily of signal transduction enzymes. *Trends Biochem. Sci.* **1997**, *22*, 1–2.
- Tallima, H.; El Ridi, R. Arachidonic acid: Physiological roles and potential health benefits - A review. *J. Adv. Res.* **2018**, *11*, 33–41.
- Dereeper, A.; Guignon, V.; Blanc, G.; Audic, S.; Buffet, S.; Chevenet, F.; Dufayard, J.-F.; Guindon, S.; Lefort, V.; Lescot, M.; Claverie, J.-M.; Gascuel, O. Phylogeny.fr: robust phylogenetic analysis for the non-specialist. *Nucleic Acids Res.* **2008**, *36*, W465–W469.
- Kalyvianaki, K.; Panagiotopoulos, A. A.; Malamos, P.; Moustou, E.; Tzardi, M.; Stathopoulos, E. N.; Ioannidis, G. S.; Marias, K.; Notas, G.; Theodoropoulos, P. A.; Castanas, E.; Kampa, M. Membrane androgen receptors (OXER1, GPRC6A AND ZIP9) in prostate and breast cancer: A comparative study of their expression. *Steroids* **2019**, *142*, 100–108.
- Stepniewski, T. M.; Torrens-Fontanals, M.; Rodríguez-Espigares, I.; Giorgino, T.; Primdahl, K. G.; Vik, A.; Stenström, Y.; Selent, J.; Hansen, T. V. Synthesis, molecular modelling studies and biological evaluation of new oxoeicosanoid receptor 1 agonists. *Bioorg. Med. Chem.* **2018**, *26*, 3580–3587.
- Kalyvianaki, K.; Gebhart, V.; Peroulis, N.; Panagiotopoulou, C.; Kiagiadaki, F.; Padiaditakis, I.; Aivaliotis, M.; Moustou, E.; Tzardi, M.; Notas, G.; Castanas, E.; Kampa, M. Antagonizing effects of membrane-acting androgens on the eicosanoid receptor OXER1 in prostate cancer. *Sci. Rep.* **2017**, *7*, No. 44418.
- Powell, W. S.; Rokach, J. Biosynthesis, biological effects, and receptors of hydroxyeicosatetraenoic acids (HETEs) and oxoeicosatetraenoic acids (oxo-ETEs) derived from arachidonic acid. *Biochim. Biophys. Acta, Mol. Cell Biol. Lipids* **2015**, *1851*, 340–355.
- Grant, G. E.; Rokach, J.; Powell, W. S. 5-Oxo-ETE and the OXE receptor. *Prostaglandins Other Lipid Mediators* **2009**, *89*, 98–104.
- Patel, P.; Cossette, C.; Anumolu, J. R.; Gravel, S.; Lesimple, A.; Mamer, O. A.; Rokach, J.; Powell, W. S. Structural Requirements for Activation of the 5-Oxo-6E,8Z,11Z,14Z-eicosatetraenoic Acid (5-Oxo-ETE) Receptor: Identification of a Mead Acid Metabolite with Potent Agonist Activity. *J. Pharmacol. Exp. Ther.* **2008**, *325*, 698–707.
- Hosoi, T.; Sugikawa, E.; Chikada, A.; Koguchi, Y.; Ohnuki, T. TG1019/OXE, a G α i/o-protein-coupled receptor, mediates 5-oxo-eicosatetraenoic acid-induced chemotaxis. *Biochem. Biophys. Res. Commun.* **2005**, *334*, 987–995.
- Powell, W. S.; Chung, D.; Gravel, S. 5-Oxo-6,8,11,14-eicosatetraenoic acid is a potent stimulator of human eosinophil migration. *J. Immunol.* **1995**, *154*, 4123–4132.
- Powell, W. S.; Gravel, S.; MacLeod, R. J.; Mills, E.; Hashefi, M. Stimulation of human neutrophils by 5-oxo-6,8,11,14-eicosatetraenoic acid by a mechanism independent of the leukotriene B4 receptor. *J. Biol. Chem.* **1993**, *268*, 9280–9286.
- Jones, C. E.; Holden, S.; Tenaillon, L.; Bhatia, U.; Seuwen, K.; Tranter, P.; Turner, J.; Kettle, R.; Bouhelal, R.; Charlton, S.; Nirmala, N. R.; Jarai, G.; Finan, P. Expression and characterization of a 5-oxo-6E,8Z,11Z,14Z-eicosatetraenoic acid receptor highly expressed on human eosinophils and neutrophils. *Mol. Pharmacol.* **2003**, *63*, 471–477.
- Takeda, S.; Yamamoto, A.; Haga, T. Identification of a G Protein-Coupled Receptor for 5-oxo-Eicosatetraenoic Acid. *Biomed. Res.* **2002**, *23*, 101–108.
- Dent, G. Leukotriene Receptors. In *xPharm: The Comprehensive Pharmacology Reference*, Enna, S. J.; Bylund, D. B., Eds.; Elsevier: New York, 2007; 1–3.
- Panagiotopoulos, A.; Papachristofi, C.; Kalyvianaki, K.; Malamos, P.; Theodoropoulos, P.; Notas, G.; Calogeropoulou, T.; Castanas, E.; Kampa, M. A simple open source bio-informatic method for initial exploration of GPCR ligands' agonistic/antagonistic properties. *Pharmacol. Res. Perspect.* **2020**, *8*, No. e00600.
- Kampa, M.; Theodoropoulou, K.; Mavromati, F.; Pelekanou, V.; Notas, G.; Lagoudaki, E. D.; Nifli, A. P.; Morel-Salmi, C.; Stathopoulos, E. N.; Vercauteren, J.; Castanas, E. Novel oligomeric proanthocyanidin derivatives interact with membrane androgen sites and induce regression of hormone-independent prostate cancer. *J. Pharmacol. Exp. Ther.* **2011**, *337*, 24–32.
- Masand, V. H.; Rastija, V. PyDescriptor: A new PyMOL plugin for calculating thousands of easily understandable molecular descriptors. *Chemom. Intell. Lab. Syst.* **2017**, *169*, 12–18.
- Gramatica, P.; Cassani, S.; Chirico, N. QSARINS-chem: Insubria datasets and new QSAR/QSPR models for environmental pollutants in QSARINS. *J. Comput. Chem.* **2014**, *35*, 1036–1044.
- Papa, E.; Kovarich, S.; Gramatica, P. On the Use of Local and Global QSPRs for the Prediction of Physico-chemical Properties of Polybrominated Diphenyl Ethers. *Mol. Inf.* **2011**, *30*, 232–240.
- Gramatica, P.; Chirico, N.; Papa, E.; Cassani, S.; Kovarich, S. QSARINS: A New Software for the Development, Analysis, and Validation of QSAR MLR Models. *J. Comput. Chem.* **2013**, *34*, 2121–2132.
- Keller, H. R.; Massart, D. L.; Brans, J. P. Multicriteria decision making: a case study. *Chemom. Int. Lab. Syst.* **1991**, *11*, 175–189.
- Katritzky, A. R.; Dobchev, D. A.; Slavov, S.; Karelson, M. Legitimate utilization of large descriptor pools for QSPR/QSAR models. *J. Chem. Inf. Model.* **2008**, *48*, 2207–2213.
- Gramatica, P.; Cassani, S.; Roy, P. P.; Kovarich, S.; Yap, C. W.; Papa, E. QSAR Modeling is not “Push a Button and Find a Correlation”: A Case Study of Toxicity of (Benzo-)triazoles on Algae. *Mol. Inf.* **2012**, *31*, 817–835.
- Southan, C.; Sharman, J. L.; Benson, H. E.; Faccenda, E.; Pawson, A. J.; Alexander, S. P.; Buneman, O. P.; Davenport, A. P.; McGrath, J. C.; Peters, J. A.; Spedding, M.; Catterall, W. A.; Fabbro, D.; Davies, J. A.; Nc, I.; et al. The IUPHAR/BPS Guide to PHARMACOLOGY in 2016: towards curated quantitative interactions between 1300 protein targets and 6000 ligands. *Nucleic Acids Res.* **2016**, *44*, D1054–D1068.
- Santos, R.; Ursu, O.; Gaulton, A.; Bento, A. P.; Donadi, R. S.; Bologa, C. G.; Karlsson, A.; Al-Lazikani, B.; Hersey, A.; Oprea, T. I.

Overington, J. P. A comprehensive map of molecular drug targets. *Nat. Rev. Drug Discov.* **2017**, *16*, 19–34.

(27) Gramatica, P. Principles of QSAR models validation: internal and external. *QSAR Comb. Sci.* **2007**, *26*, 694–701.

(28) Gore, V.; Gravel, S.; Cossette, C.; Patel, P.; Chourey, S.; Ye, Q.; Rokach, J.; Powell, W. S. Inhibition of 5-Oxo-6,8,11,14-eicosate-traenoic Acid-Induced Activation of Neutrophils and Eosinophils by Novel Indole OXE Receptor Antagonists. *J. Med. Chem.* **2014**, *57*, 364–377.

(29) Gore, V.; Patel, P.; Chang, C. T.; Sivendran, S.; Kang, N.; Ouedraogo, Y. P.; Gravel, S.; Powell, W. S.; Rokach, J. 5-Oxo-ETE receptor antagonists. *J. Med. Chem.* **2013**, *56*, 3725–3732.

(30) Sterling, T.; Irwin, J. J. ZINC 15—Ligand Discovery for Everyone. *J. Chem. Inf. Model.* **2015**, *55*, 2324–2337.

(31) Daina, A.; Michielin, O.; Zoete, V. SwissADME: a free web tool to evaluate pharmacokinetics, drug-likeness and medicinal chemistry friendliness of small molecules. *Sci. Rep.* **2017**, *7*, No. 42717.

(32) Benet, L. Z.; Hosey, C. M.; Ursu, O.; Oprea, T. I. BDDCS, the Rule of 5 and drugability. *Adv. Drug Deliv. Rev.* **2016**, *101*, 89–98.

(33) Lipinski, C. A.; Lombardo, F.; Dominy, B. W.; Feeney, P. J. Experimental and computational approaches to estimate solubility and permeability in drug discovery and development settings. *Adv. Drug Deliv. Rev.* **2001**, *46*, 3–26.

(34) Keiser, M. J.; Roth, B. L.; Armbruster, B. N.; Ernsberger, P.; Irwin, J. J.; Shoichet, B. K. Relating protein pharmacology by ligand chemistry. *Nat. Biotechnol.* **2007**, *25*, 197–206.

(35) Lee, G. R.; Seok, C. Galaxy7TM: flexible GPCR-ligand docking by structure refinement. *Nucleic Acids Res.* **2016**, *44*, W502–W506.

(36) Senior, A. W.; Evans, R.; Jumper, J.; Kirkpatrick, J.; Sifre, L.; Green, T.; Qin, C.; Zidek, A.; Nelson, A. W. R.; Bridgland, A.; Penedones, H.; Petersen, S.; Simonyan, K.; Crossan, S.; Kohli, P.; Jones, D. T.; Silver, D.; Kavukcuoglu, K.; Hassabis, D. Improved protein structure prediction using potentials from deep learning. *Nature* **2020**, *577*, 706–710.

(37) Senior, A. W.; Evans, R.; Jumper, J.; Kirkpatrick, J.; Sifre, L.; Green, T.; Qin, C.; Zidek, A.; Nelson, A. W. R.; Bridgland, A.; Penedones, H.; Petersen, S.; Simonyan, K.; Crossan, S.; Kohli, P.; Jones, D. T.; Silver, D.; Kavukcuoglu, K.; Hassabis, D. Protein structure prediction using multiple deep neural networks in the 13th Critical Assessment of Protein Structure Prediction (CASP13). *Proteins* **2019**, *87*, 1141–1148.

(38) Yang, J.; Roy, A.; Zhang, Y. Protein-ligand binding site recognition using complementary binding-specific substructure comparison and sequence profile alignment. *Bioinformatics* **2013**, *29*, 2588–2595.

(39) Nifli, A. P.; Bosson-Kouame, A.; Papadopoulou, N.; Kogia, C.; Kampa, M.; Castagnino, C.; Stournaras, C.; Vercauteren, J.; Castanas, E. Monomeric and oligomeric flavanols are agonists of membrane androgen receptors. *Exp. Cell Res.* **2005**, *309*, 329–339.

(40) Hosoi, T.; Koguchi, Y.; Sugikawa, E.; Chikada, A.; Ogawa, K.; Tsuda, N.; Suto, N.; Tsunoda, S.; Taniguchi, T.; Ohnuki, T. Identification of a novel human eicosanoid receptor coupled to G(i/o). *J. Biol. Chem.* **2002**, *277*, 31459–31465.

(41) Thomas, P. Membrane Androgen Receptors Unrelated to Nuclear Steroid Receptors. *Endocrinology* **2019**, *160*, 772–781.

(42) Sarveswaran, S.; Ghosh, J. OXER1, a G protein-coupled oxoeicosatetraenoic acid receptor, mediates the survival-promoting effects of arachidonate 5-lipoxygenase in prostate cancer cells. *Cancer Lett.* **2013**, *336*, 185–195.

(43) Sundaram, S.; Ghosh, J. Expression of 5-oxoETE receptor in prostate cancer cells: critical role in survival. *Biochem. Biophys. Res. Commun.* **2006**, *339*, 93–98.

(44) Hatzoglou, A.; Kampa, M.; Kogia, C.; Charalampopoulos, I.; Theodoropoulos, P. A.; Anezinis, P.; Dambaki, C.; Papakonstanti, E. A.; Stathopoulos, E. N.; Stournaras, C.; Gravanis, A.; Castanas, E. Membrane androgen receptor activation induces apoptotic regression of human prostate cancer cells in vitro and in vivo. *J. Clin. Endocrinol. Metab.* **2005**, *90*, 893–903.

(45) Gramatica, P. Principles of QSAR Modeling: Comments and Suggestions From Personal Experience. *Int. J. Quant. Struct.-Prop. Relat.* **2020**, *5*, 1–37.

(46) Aller, S. G.; Yu, J.; Ward, A.; Weng, Y.; Chittaboina, S.; Zhuo, R.; Harrell, P. M.; Trinh, Y. T.; Zhang, Q.; Urbatsch, I. L.; Chang, G. Structure of P-glycoprotein reveals a molecular basis for poly-specific drug binding. *Science* **2009**, *323*, 1718–1722.

(47) Wolking, S.; Schaeffeler, E.; Lerche, H.; Schwab, M.; Nies, A. T. Impact of Genetic Polymorphisms of ABCB1 (MDR1, P-Glycoprotein) on Drug Disposition and Potential Clinical Implications: Update of the Literature. *Clin. Pharmacokinet.* **2015**, *54*, 709–735.

(48) Rettie, A. E.; Jones, J. P. Clinical and toxicological relevance of CYP2C9: drug-drug interactions and pharmacogenetics. *Annu. Rev. Pharmacol. Toxicol.* **2005**, *45*, 477–494.

(49) Pelekanou, V.; Notas, G.; Sanidas, E.; Tsapis, A.; Castanas, E.; Kampa, M. Testosterone membrane-initiated action in breast cancer cells: Interaction with the androgen signaling pathway and EPOR. *Mol. Oncol.* **2010**, *4*, 135–149.

(50) Kampa, M.; Pelekanou, V.; Castanas, E. Membrane-initiated steroid action in breast and prostate cancer. *Steroids* **2008**, *73*, 953–960.

(51) Kampa, M.; Kogia, C.; Theodoropoulos, P. A.; Anezinis, P.; Charalampopoulos, I.; Papakonstanti, E. A.; Stathopoulos, E. N.; Hatzoglou, A.; Stournaras, C.; Gravanis, A.; Castanas, E. Activation of membrane androgen receptors potentiates the antiproliferative effects of paclitaxel on human prostate cancer cells. *Mol. Cancer Ther.* **2006**, *5*, 1342–1351.

(52) Zendah, I.; Riaz, N.; Nasr, H.; Frauendorf, H.; Schuffler, A.; Raies, A.; Laatsch, H. Chromophenazines from the terrestrial Streptomyces sp. Ank 315. *J. Nat. Prod.* **2012**, *75*, 2–8.

(53) Mavrodi, D. V.; Bonsall, R. F.; Delaney, S. M.; Soule, M. J.; Phillips, G.; Thomashow, L. S. Functional analysis of genes for biosynthesis of pyocyanin and phenazine-1-carboxamide from *Pseudomonas aeruginosa* PAO1. *J. Bacteriol.* **2001**, *183*, 6454–6645.

(54) Handelsman, J.; Stabb, E. V. Biocontrol of Soilborne Plant Pathogens. *Plant Cell* **1996**, *8*, 1855–1869.

(55) Choi, S. R.; Lim, J. H.; Kim, M. Y.; Kim, E. N.; Kim, Y.; Choi, B. S.; Kim, Y. S.; Kim, H. W.; Lim, K. M.; Kim, M. J.; Park, C. W. Adiponectin receptor agonist AdipoRon decreased ceramide, and lipotoxicity, and ameliorated diabetic nephropathy. *Metabolism* **2018**, *85*, 348–360.

(56) Grandhaye, J.; Hmadeh, S.; Plotton, I.; Levasseur, F.; Estienne, A.; LeGuevel, R.; Levern, Y.; Rame, C.; Jeanpierre, E.; Guerif, F.; Dupont, J.; Froment, P. The adiponectin agonist, AdipoRon, inhibits steroidogenesis and cell proliferation in human luteinized granulosa cells. *Mol. Cell. Endocrinol.* **2021**, *520*, No. 111080.

(57) Ramzan, A. A.; Bitler, B. G.; Hicks, D.; Barner, K.; Qamar, L.; Behbakht, K.; Powell, T.; Jansson, T.; Wilson, H. Adiponectin receptor agonist AdipoRon induces apoptotic cell death and suppresses proliferation in human ovarian cancer cells. *Mol. Cell. Biochem.* **2019**, *461*, 37–46.

(58) Malih, S.; Najafi, R. AdipoRon: a possible drug for colorectal cancer prevention? *Tumour Biol.* **2015**, *36*, 6673–6675.

(59) Akimoto, M.; Maruyama, R.; Kawabata, Y.; Tajima, Y.; Takenaga, K. Antidiabetic adiponectin receptor agonist AdipoRon suppresses tumour growth of pancreatic cancer by inducing RIPK1/ERK-dependent necroptosis. *Cell Death Dis.* **2018**, *9*, No. 804.

(60) Cai, Y.; Fredenhagen, A.; Hug, P.; Meyer, T.; Peter, H. H. Further minor metabolites of staurosporine produced by a *Streptomyces longisporoflavus* strain. *J. Antibiot.* **1996**, *49*, 519–526.

(61) Rostom, S. A.; Hassan, G. S.; El-Subbagh, H. I. Synthesis and biological evaluation of some polymethoxylated fused pyridine ring systems as antitumor agents. *Arch. Pharm.* **2009**, *342*, 584–590.

(62) Yang, J. M.; Chen, C. C. GEMDOCK: a generic evolutionary method for molecular docking. *Proteins* **2004**, *55*, 288–304.

(63) Wen, A. Y.; Sakamoto, K. M.; Miller, L. S. The role of the transcription factor CREB in immune function. *J. Immunol.* **2010**, *185*, 6413–6419.

- (64) Biasini, M.; Bienert, S.; Waterhouse, A.; Arnold, K.; Studer, G.; Schmidt, T.; Kiefer, F.; Gallo Cassarino, T.; Bertoni, M.; Bordoli, L.; Schwede, T. SWISS-MODEL: modelling protein tertiary and quaternary structure using evolutionary information. *Nucleic Acids Res.* **2014**, *42*, W252–W258.
- (65) Arnold, K.; Bordoli, L.; Kopp, J.; Schwede, T. The SWISS-MODEL workspace: a web-based environment for protein structure homology modelling. *Bioinformatics* **2006**, *22*, 195–201.
- (66) O'Boyle, N. M.; Banck, M.; James, C. A.; Morley, C.; Vandermeersch, T.; Hutchison, G. R. Open Babel: An open chemical toolbox. *J. Cheminform.* **2011**, *3*, No. 33.
- (67) Lee, G. R.; Heo, L.; Seok, C. Effective protein model structure refinement by loop modeling and overall relaxation. *Proteins* **2016**, *84*, 293–301.
- (68) Heo, L.; Park, H.; Seok, C. GalaxyRefine: Protein structure refinement driven by side-chain repacking. *Nucleic Acids Res.* **2013**, *41*, W384–W388.
- (69) Pettersen, E. F.; Goddard, T. D.; Huang, C. C.; Couch, G. S.; Greenblatt, D. M.; Meng, E. C.; Ferrin, T. E. UCSF Chimera—a visualization system for exploratory research and analysis. *J. Comput. Chem.* **2004**, *25*, 1605–1612.
- (70) Macindoe, G.; Mavridis, L.; Venkatraman, V.; Devignes, M. D.; Ritchie, D. W. HexServer: an FFT-based protein docking server powered by graphics processors. *Nucleic Acids Res.* **2010**, *38*, W445–W449.
- (71) Heo, L.; Park, S.; Seok, C. GalaxyWater-wKGB: Prediction of Water Positions on Protein Structure Using wKGB Statistical Potential. *J. Chem. Inf. Model.* **2021**, *61*, 2283–2293.
- (72) Todeschini, R.; Consonni, V.; Maiocchi, A. The K correlation index: theory development and its application in chemometrics. *Chemom. Int. Lab. Syst.* **1999**, *46*, 13–29.
- (73) Haupt, R. L.; Haupt, S. E. *Practical Genetic Algorithms*, 2nd ed.; Wiley-Interscience: New Jersey, United States, 2004.
- (74) Rogers, D.; Hopfinger, A. J. Application of genetic function approximation to quantitative structure–activity relationships and quantitative structure–property relationships. *J. Chem. Inf. Comput. Sci.* **1994**, *34*, 854–866.